A 1x4 Focal Plane Array Using 230 GHz SIS Mixers

John Garrett[1,*], Jamie Leech[1], Faouzi Boussaha[2], Christine Chaumont[2], Brian Ellison[3], and Ghassan Yassin[1]

[1]*University of Oxford, Oxford, U.K.*

[2]*GEPI, Observatoire de Paris, Paris, France*

[3] *Rutherford Appleton Laboratory, U.K.*

*Contact: john.garrett@physics.ox.ac.uk

***Abstract*—A new 1x4 focal plane array centered around 230 GHz is presented in this paper. The size of the array was limited to 4 pixels due to the space available in the test cryostat; however, we can expand the design in the future. On the front of the array block there are 4 waveguides flanges for the RF feed horns, while the local-oscillator signal enters through a separate waveguide on the side. The local-oscillator power is multiplexed using cascaded E-plane power dividers and then combined with the RF signals using directional couplers. Preliminary tests of the array block have now been completed. They show reasonable local-oscillator distribution and excellent RF signal isolation. Future work will involve testing the noise properties of the array block and improving the local-oscillator distribution.**

I. Introduction

A common application of millimeter-wave receivers is observing molecular transitions in star forming regions. We would like to map these regions to understand their physical and chemical properties; however, from our perspective, these regions can extend over very large angular diameters (~0<θ<~100 arcmin). Large surveys are slow using single dish antennas and even more difficult with interferometers due to their inherently narrow beam widths. Unfortunately, increasing the mapping speed of heterodyne receivers around 230 GHz is very challenging because the current state-of-the-art Superconductor/Insulator/Superconductor (SIS) receivers are already very close the quantum limit sensitivity. This means that any further improvements to sensitivity (and therefore mapping speed) will be modest.

An alternative technique to improve the mapping speed is to increase the number of receivers in the focal plane. The mapping speed of a focal plane array is proportional to

$$\frac{N}{{T_n}^2} \qquad (1)$$

where N is the number of pixels in the array, and T_n is the system noise temperature. The challenge then is to add more pixels without increasing the noise temperature. Two general approaches are to (a) create a large number of pixels with relatively poor noise properties, or (b) create a modest number of pixels with very good noise properties. The latter is more desirable due to the lower requirements on the backend of the receiver.

Perhaps the most obvious challenge in creating a focal plane array is the complexity since more pixels require more feed horns, low noise amplifiers (LNAs), magnetic coils, bias wires, etc. All of these components are required to fit into a very compact space, and for older telescopes, this often means fitting into a space that was only ever intended for a single pixel receiver. (A side effect of the complexity is also the added thermal load due to the additional wiring and LNAs.)

Another major challenge comes from efficiently pumping all of the SIS devices. The local-oscillator (LO) signal has to be evenly divided amongst the pixels (i.e., multiplexed) and then injected into each SIS device (i.e., diplexed) without interfering with the RF signal path. SIS mixers are relatively insensitive to LO power (compared to HEBs), but it is important to keep Eqn. (1) in mind to balance the cost/benefit of adding more pixels. Most of the other focal plane arrays around 230 GHz use waveguide power splitters to divide the LO signal (e.g., HERA [1] and SuperCam [2]). Alternatively, the NRAO 8-beam array used cascaded wire grids [3], DesertStar used a reflective phase grating [4] and HARP-B uses a freespace meander line [5], but these techniques either become very complex above ~16 pixels or they limit the RF bandwidth of the receiver. In order to combine the LO and RF signals, SuperCam, HARP-B and DesertStar all use Mylar beam splitters; however, this complicates the telescope's optics since they require additional alignment. At frequencies below ~400 GHz, waveguide directional couplers, such as those used by HERA, are likely a better option.

In this paper, we present a new 1x4 focal plane array centered around 230 GHz. The array uses waveguide power splitters to divide the LO signal and directional couplers to inject the LO signals into the RF waveguides. These techniques facilitate the optical system since no freespace components are required for the LO. This should allow the design to be expanded into a much larger format in the future.

II. Design

A 3D render of the 1x4 array is shown in Fig. 1. The waveguide flanges for the four pixels are seen on the front of the array block and one flange is visible on the side for the LO signal (Fig. 1a). Spindles for the magnetic coils are also visible on top of the block with soft iron pole pieces to direct the magnetic field across the SIS devices. The size of the new focal plane array was limited to 1x4 due to the space available in our test cryostat. This array will act as a demonstrator to test our new design and then it can be expanded in the future. This may include expanding the array into a larger linear strip, such as 1x8, and then stacking the strips to form an 8x8 focal plane array, similar to SuperCam.

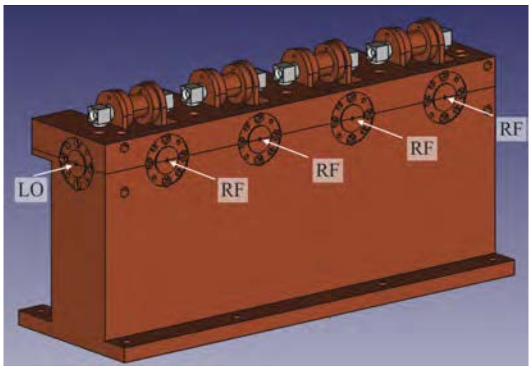

(a) The array block fully assembled.

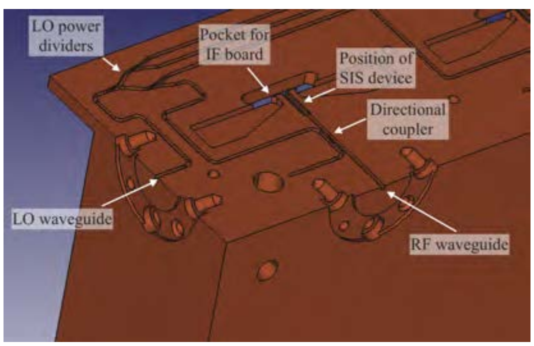

(b) The bottom half of the array block (top half removed).

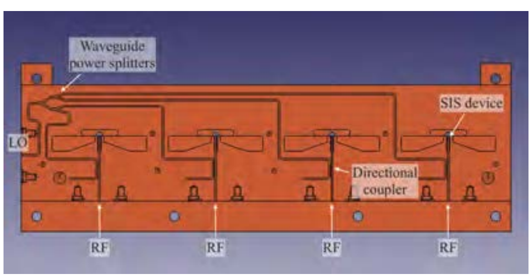

(c) The entire lower half of the array block.

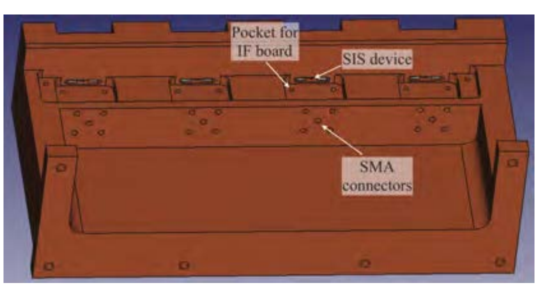

(d) The lower half of the array block showing where the IF boards are placed to route the IF signal downwards.

Fig. 1. Design of the 1x4 focal plane array block.

The waveguides were machined using split-block fabrication. In Fig. 1b, the upper half is removed to display the inner waveguides. As the LO signal enters the array block from the left-hand side, it is first divided in four using cascaded E-plane power splitters, and then the LO signal is injected into each RF waveguide using a direction coupler. The entire lower half of the array block is shown in Fig. 1c. Since the RF and LO waveguides are in the same plane, the IF signal is routed downwards to avoid any crossover, as shown in Fig. 1d. An IF tuning board sits in the pocket on the back of the array block, which connects the SIS device to an SMA connector (not shown in Fig. 1d).

A. Bow-tie couplers

The directional couplers were designed using bow tie antennas (Fig. 2a). These couplers are similar to the couplers that were previously used by the GUBBINS system [6]. The coupling was optimized using HFSS simulations to be approximately -17 dB (Fig. 2b); although, past experience from the GUBBINS system suggests that the actual coupling could be closer to -13 dB.

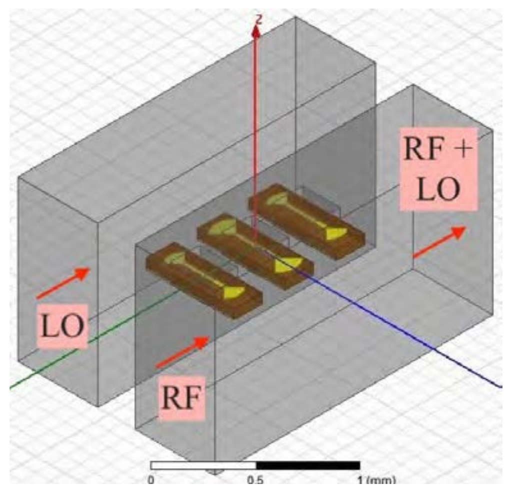

(a) Bow-tie antennas used as cross-guide couplers.

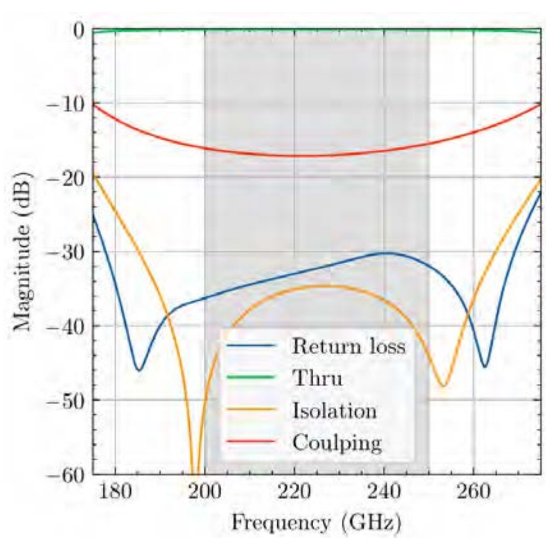

(b) Simulated performance from HFSS.

Fig. 2. Waveguide directional coupler using bow-tie antennas.

B. E-plane waveguide power splitters

As seen previously in Fig. 1b, the LO power is divided using cascaded E-plane power splitters. The 3D model of one of these power splitters is shown in Fig. 3a. The design was optimized to provide less than -15 dB of return loss from 200 GHz to 280 GHz (Fig. 3b).

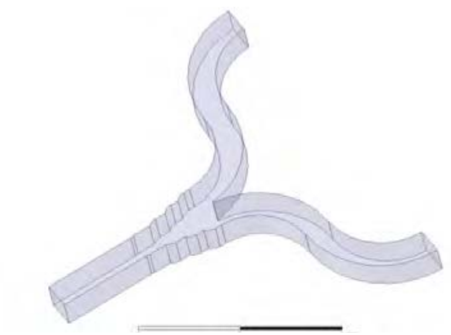

(a) 3D rendering of one of the power splitters.

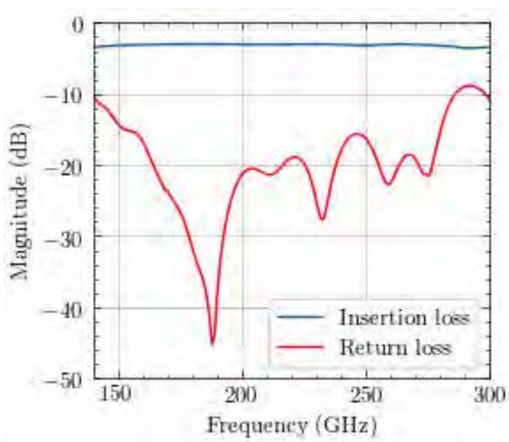

(b) Simulated performance of the power splitters.

Fig. 3. -3dB E-plane power splitters.

III. 230 GHz Mixer Device

The SIS device that was installed inside the array block has already been reported in [7,8]. It is a single-ended device that uses a finline transition to couple the RF and LO signals from the waveguide to the planar circuit. The device was fabricated on a 100 µm quartz substrate with a 1.5 µm^2 Nb/Al-AlO$_x$/Nb SIS junction. It was designed to operate from 140 to 260 GHz with an IF range from DC to +12 GHz.

This SIS device has been tested extensively in a single pixel mixer block. The SIS junction exhibits excellent DC properties with a typical quality factor of $Q = R_{sg}/R_n > 30$ and a current density of J_c~13.7 kA/cm^2. Using an LO with a 213-257 GHz tuning range, excellent RF performance was found from 215 to 245 GHz, with a noise temperature close to 40 K (Fig. 4). The IF response spans from DC to 12 GHz, although the noise temperature quickly degrades past ~8 GHz.

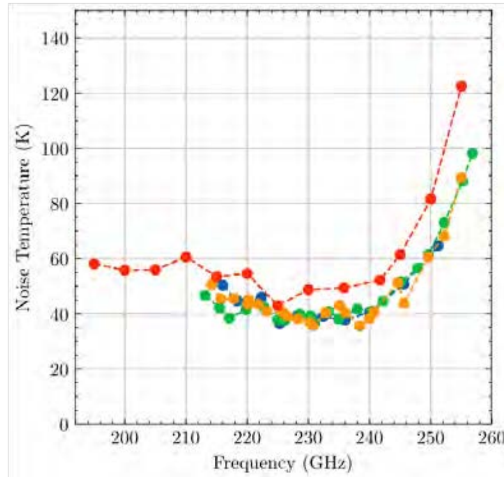

Fig. 4. Measured RF performance from the 230 GHz SIS device in a single mixer block. The different colors represent different devices. The device represented by the red line was tested with a different LO that has a wider tuning range but worse noise properties, which is why the noise temperature of this device is ~10 K higher than the others.

IV. Fabrication and Assembly

The array block was manufactured at the Rutherford Appleton Laboratory (RAL) Space Precision Design Facility. All of the components were machined from high quality copper except for the magnetic pole pieces which were machined from soft iron. The finished array can be seen in Fig. 5. Note that highly precise machining was required for the power dividers (Fig. 5b).

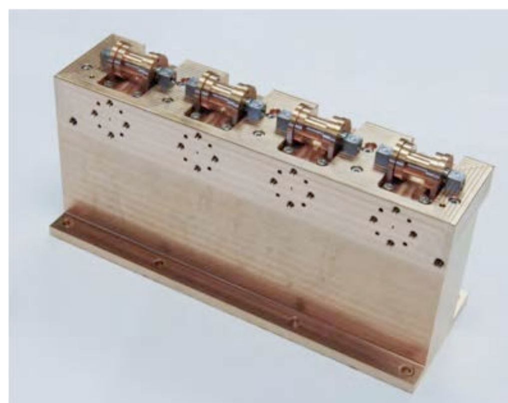

(a) The assembled array block.

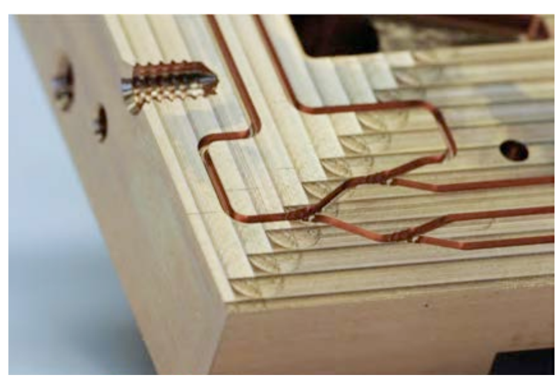

(b) The waveguide power dividers.

Fig. 5. Photos of the finished array block.

A. IF boards

In the original design, the IF boards were meant to be installed vertically at a 90° angle to the SIS device (see Fig. 1d). In practice, however, it was too difficult to attach the bond wires over the 90° corner. Instead, the IF board was printed onto a flexible substrate (DuPont™ Pyralux® TK1810018R), so that it could bend over the corner. This allowed one end of the IF board to be in the same plane as the SIS device, making the wire bonding much easier. Although the flexible substrate has higher attenuation than Duroid®, the insertion loss was measured to be less than 1 dB at 20 GHz (for a 3 cm long 50 Ω microstrip).

B. Directional couplers

When the array block was first fabricated, the directional couplers were machined in the wrong direction (see Fig. 1b). To fix this error, the old waveguides were drilled out and then filled back in with copper slugs. This allowed the directional couplers to be re-machined. Unfortunately, at the time, no CNC milling machines were available. The new waveguide bend then needed a new machining technique that only required straight cuts. The solution, shown in Fig. 6a, was to leave a small amount of material in the outside corner. HFSS simulations showed excellent performance from 150 to 270 GHz (Fig. 6b).

(a) A cross-section of the new waveguide bend design.

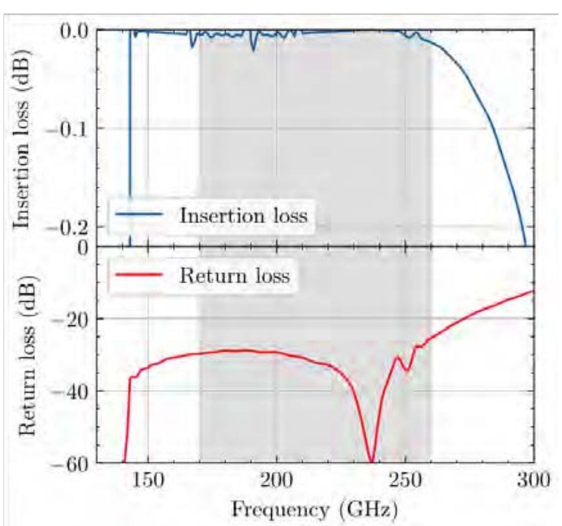

(b) Simulated performance from HFSS. The gray region is the standard frequency range for aWR4.3 waveguide (170-260 GHz).

Fig. 6. An E-plane waveguide bend that can be machined using a drill bit that is the diameter of the waveguide's minor axis and using a milling machine that can only make straight cuts (i.e., not a CNC milling machine).

V. Preliminary Test Results

For the preliminary tests, the array block was installed into the open-cycle cryostat shown in Fig. 7. Since this cryostat has had difficulties cooling in the past, only two windows were installed on the front of the cryostat to limit the radiative heat load. This allowed for freespace coupling for the LO signal and one RF pixel. Since each pixel is identical, each pixel should also have the same noise properties, provided that the LO pumping level is similar. Even though only one pixel could see outside the cryostat, all of the other pixels were still connected to DC bias supplies and current sources for the magnetic coils. This allowed us to measure the I-V curves from all of the pixels, from which we could recover the pumping levels. This setup allowed us to test the LO distribution and RF signal isolation.

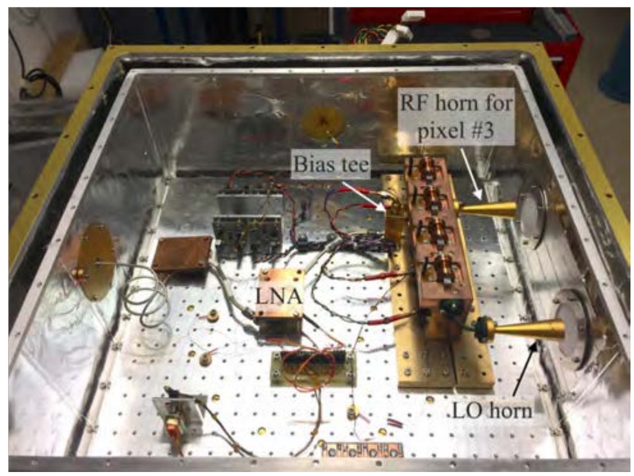

Fig. 7. The 1x4 focal plane array installed in the test cryostat. Only two windows were used for the initial tests. This allowed for freespace coupling for the LO signal and pixel #3.

A. LO distribution

In any focal plane array, it is important that the LO power is evenly distributed between the pixels in order to pump each SIS device to the optimum level. Otherwise, if the pumping level of some of the pixels is lower than others, the conversion gains of those pixels will be lower, resulting in higher IF noise contributions and therefore lower sensitivities.

To test the LO distribution, the LO signal was injected into the LO port of the array block, and then the pumped and unpumped I–V curves were measured from each pixel. The junction drive level and the power delivered to each SIS junction was then recovered by comparing the pumped and unpumped I-V curves. With the LO set to 230 GHz, the recovered junction drive levels were $\alpha_1 = 0.80$, $\alpha_2 = 0.72$, $\alpha_3 = 1.07$, and $\alpha_4 = 0.55$ (where $\alpha = V_J/V_{ph}$, V_J is the voltage across the junction, and V_{ph} is the equivalent photon voltage). Based on how the noise temperature changes with the drive level in the single pixel mixer block (Fig. 8), these drive levels roughly correspond to noise temperatures of $T_{n1} = 43.1$ K, $T_{n2} = 46.2$ K, $T_{n3} = 40.2$ K, and $T_{n4} = 57.4$ K. Although, this distribution is not ideal, it does result in adequate noise properties. The noise temperatures could be improved by over-saturating some of the pixels (i.e., driving some of the pixels past $\alpha \sim 1$) since the noise temperature does not deteriorate very much past the saturation point.

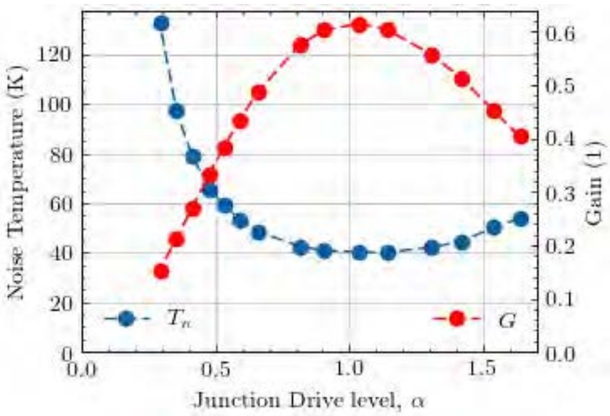

Fig. 8. Noise and gain performance compared to the junction drive level. This data was measured using a single pixel mixer block.

B. RF signal isolation

The RF signal isolation is a measure of the signal leakage between adjacent pixels. Typically isolation is measured by injecting a strong signal into one of the pixels, and then comparing the IF outputs from the surrounding pixels. However, in the current test setup, none of the pixels are connected to an IF backend. Instead, the signal isolation was measured by injecting a strong LO tone into pixel #3, and then measuring the pumped and unpumped I-V curves from the other pixels. Similar to the LO distribution test, this allowed us to recover the junction drive levels.

When this test was performed at 230 GHz, pixel #3 was pumped to $\alpha_3 = 1.624$. The pump levels of the surrounding pixels were then measured to be $\alpha_1 = 0.045$, $\alpha_2 = 0.048$ and $\alpha_4 = 0.046$. Since the junction drive level is proportional to the voltage across the junction, the signal isolation between the 3rd pixel and the *i*th pixel was then calculated by

$$I_{i,3} = -20 \cdot \log_{10}\left({}^{\alpha_i}/{}_{\alpha_3}\right).$$

For the drive levels listed above, this corresponds to isolation levels of $I_{1,3} = 31.1$ dB, $I_{2,3} = 30.6$ dB, and $I_{4,3} = 31.0$ dB. This is a very good level of isolation since less than 1/1000th of the signal power of pixel #3 leaked into the adjacent pixels.

VI. Future Work

The next step for this project will involve connecting the focal plane array to an IF measurement chain and then measuring the response to hot and cold black body loads to characterize the noise temperature and gain. The LO distribution could potentially be improved by repositioning some of the bow-tie antennas.

Conclusions

A new 1x4 focal plane array has been presented. It uses waveguide power splitters to divide the LO signal and a waveguide coupler based on bow-tie antennas to combine the LO and RF signals. Preliminary results show reasonable LO distribution and very good LO isolation. Future work will involve testing the noise properties of the array, and potentially expanding the array design to a larger format, such 8x8.

Acknowledgment

We would like to thank Mat Beardsley (RAL Space) for fabricating the array block, Byron Alderman (STFC/Teratech Components Ltd.) for fabricating the bow tie antennas, and Nick Brewster (STFC) for his assistance installing the bow-ties.

References

[1] K.-F. Schuster, *et al.*, "A 230 GHz heterodyne receiver array for the IRAM 30 m telescope," *Astronomy & Astrophysics*, vol. 423, no. 3, pp. 1171–1177, Sep. 2004.

[2] C. Groppi, *et al.*, "SuperCam: A 64 pixel heterodyne array receiver for the 350 GHz Atmospheric Window," in *Proc. 20th Int. Symp. Space THz Tech.*, Charlottesville, 2009, pp. 90–96.

[3] J. Payne and P. Jewell, "The Upgrade of the NRAO 8-beam receiver," in *ASP Conf. Series*, vol. 75, 1995, pp. 114–148.

[4] C. E. Groppi, *et al.*, "DesertSTAR: a 7 pixel 345 GHz heterodyne array receiver for the Heinrich Hertz Telescope," in *Proc. of SPIE (vol. 4855)*, Marseille, France, 2003, p. 330-337.

[5] H. Smith, *et al.*, "HARP: a submillimeter heterodyne array receiver operating on the James Clerk Maxwell Telescope," in *Proc. of SPIE (vol. 4855)*, Marseille, France, 2003, pp. 338–348.

[6] P. Grimes, *et al.*, "GUBBINS: A novel millimeter-wave heterodyne interferometer," in *Proc. 20th Int. Symp. Space THz Tech.*, Charlottesville, VA, Apr. 2009.

[7] J. Garrett, B.K. Tan, F. Boussaha, C. Chaumont, and G. Yassin, "A 220 GHz Finline Mixer with Ultra-Wide Instantaneous Bandwidth," in *Proc. 26th Int. Symp. Space THz Tech.*, Cambridge, MA, Mar. 2015.

[8] J. Garrett, F. Boussaha, C. Chaumont, B.K. Tan, and G. Yassin, "A 230 GHz finline SIS receiver with wide IF bandwidth," in *Proc. 27th Int. Symp. Space THz Tech.*, Nanjing, China, Mar. 2016.